THE JOURNAL OF PHYSICAL CHEMISTRY B

ARTICLE

pubs.acs.org/JPCB

PEG and mPEG−Anthracene Induce DNA Condensation and Particle Formation

E. Froehlich,[†] J. S. Mandeville,[†] D. Arnold,[‡] L. Kreplak,[‡] and H. A. Tajmir-Riahi*[,†]

[†]Department of Chemistry-Biology, University of Québec at Trois-Rivières, C.P. 500, Trois-Rivières (Québec), Canada G9A 5H7

[‡]Department of Physics, Sir James Dunn Building, Dalhousie University, Lord Dalhousie Drive, Halifax, Canada NS B3H 3J5

ABSTRACT: In this study, we investigated the binding of DNA with poly(ethylene glycol) (PEG) of different sizes and compositions such as PEG 3350, PEG 6000, and mPEG−anthracene in aqueous solution at physiological conditions. The effects of size and composition on DNA aggregation and condensation as well as conformation were determined using Fourier transform infrared (FTIR), UV−visible, CD, fluorescence spectroscopic methods and atomic force microscopy (AFM). Structural analysis showed moderate complex formation for PEG 3350 and PEG 6000 and weaker interaction for mPE−anthracene−DNA adducts with both hydrophilic and hydrophobic contacts. The order of ± stability of the complexes formed is $K_{PEG\ 6000}$ = 1.5 (±0.4) × 10^4 M^{-1} > $K_{PEG\ 3350}$ = 7.9 (±1) × 10^3 M^{-1} > $K_{m_{PEG-anthracene}}$ = 3.6 (±0.8) × 10^3 M^{-1} with nearly 1 bound PEG molecule per DNA. No B−DNA conformational changes were observed, while DNA condensation and particle formation occurred at high PEG concentration.

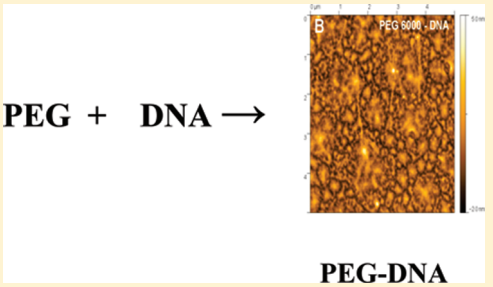

INTRODUCTION

In constant search to design and develop tool for gene and drug delivery, polymers play a major role as vehicles for transportation. Among synthetic polymers, poly(ethylene glycol) (PEG) and its derivatives show potential applications in gene delivery due to their solubility, nontoxicity and biocompatibility.[1,2] PEGylation of synthetic polymers such as dendrimers is shown to reduce toxicity and increase biocompatibility and DNA transfection.[3−6] Similarly, the effect of PEGylation on the toxicity and permeability of biopolymers such as chitosan has been reported.[7] It has been reported that PEG induces significant changes in DNA solubility and structure under given conditions. DNA concentration, pH, ionic strength of the solution and the presence of divalent metal cations have been shown to impact PEG−DNA precipitation.[8,9] The differences between PEG and copolymers such as triblock poly(ethylenoxide)−propylene oxide−poly(ethylene oxide) (PEO−PPO−PEO) on DNA complexation and transfection efficiency have been explored and it is shown that DNA condensation occurs even at low PEG concentration compared to copolymers.[1] Even though, the interactions of PEGylated dendrimers with DNA, RNA and protein are well characterized,[10−13] detailed structural analysis of PEG and mPEG derivatives complexes with DNA are not known. Therefore, it was of interest to examine the interaction of PEGs and mPEG−anthracene with DNA, using spectroscopic methods and AFM measurements.

Fluorescence quenching has been used as a convenient technique for quantifying the binding affinities of macromolecules with ligands.[14] Fluorescence quenching is the decrease of the quantum yield of fluorescence from a fluorophore induced by a variety of molecular interactions with a quencher molecule. Therefore, it is possible to use quenching of the m-PEG−anthracene as a tool to study the interaction of PEG with DNA in an attempt to characterize the nature of polymer−DNA complexation.

In this report we analyze the interaction of calf-thymus DNA with PEG 3350, PEG 6000, and mPEG−anthracene in aqueous solution at physiological conditions using different polymer concentrations and constant DNA content. FTIR, CD, and UV−visible and fluorescence spectroscopic methods as well as atomic force microscopy (AFM) were used to locate the binding site, the overall binding constant and the DNA condensation and particle formation in the PEG−DNA adducts.

MATERIALS AND METHODS

Materials. Highly polymerized type I calf-thymus DNA sodium salt (7% Na content) was purchased from Sigma Chemical Co., and was deproteinated by the addition of $CHCl_3$ and isoamyl alcohol in NaCl solution. In order to check the protein content of DNA solution, the absorbance at 260 and 280 nm was recorded. The A_{260}/A_{280} ratio was 1.85, showing that the DNA was sufficiently free from protein. PEG 3350 and PEG 6000 were purchased form Aldrich Chemical Co and used as supplied. m-PEG−anthracene was from Polymer Source (Quebec). Other chemicals were of reagent grade and used without further purification.

Preparation of Stock Solution. Sodium−DNA was dissolved to 1% w/w (10 mg/mL) in 10 mL Tris−HCl (pH 7.3) at 5 °C for 24 h with occasional stirring to ensure the

Received: May 31, 2011
Revised: June 26, 2011
Published: July 18, 2011

formation of a homogeneous solution. The final concentration of the stock calf-thymus DNA solution was determined spectrophotometrically at 260 nm by using molar extinction coefficient of 6600 cm^{-1} M^{-1} (expressed as molarity of phosphate groups).[15,16] The UV absorbance at 260 nm of a diluted solution (40 μM) of calf-thymus DNA used in our experiments was measured to be 0.25 (path length was 1 cm) and the final concentration of the stock DNA solution was calculated to be 25 mM in DNA phosphate. The average length of the DNA molecules, estimated by gel electrophoresis, was 9000 base pairs (molecular weight $\sim 6 \times 10^6$ Da). The appropriate amount of PEG and its derivatives (0.25 to 2 mM) was prepared in distilled water and diluted in Tris−HCl The PEG solution was then added dropwise to DNA solution.

FTIR Spectroscopy. Infrared spectra were recorded on a FTIR spectrometer (Impact 420 model), equipped with DTGS (deuterated triglycine sulfate) detector and KBr beam splitter, using AgBr windows. Spectra were collected after 2 h incubation of PEG with DNA solution and measured in triplicate. The PEG concentrations used in infrared were 0.125, 0.25, 0.5, and 1 mM with final DNA content of 12.5 mM (P). Interferograms were accumulated over the spectral range 4000−400 cm^{-1} with a nominal resolution of 2 cm^{-1} and a minimum of 100 scans. The water subtraction was carried out with 0.1 mM NaCl solution used as a reference at pH 7.3.[17] A good water subtraction was achieved as shown by a flat baseline around 2200 cm^{-1} where the water combination mode is located. This method is a rough estimate, but removes the water content in a satisfactory way. The difference spectra [(DNA solution + PEG solution) − (DNA solution)] were obtained, using the sharp DNA band at 968 cm^{-1} as internal reference. This band, which is due to deoxyribose C−C stretching vibration, exhibits no spectral changes (shifting or intensity variation) upon polymer−DNA complexation, and canceled out upon spectral subtraction. The spectra are smoothed with the Savitzky−Golay procedure.[17]

The plots of the relative intensity (R) of several peaks of DNA in-plane vibrations related to A-T, G-C base pairs and the PO_2^- stretching vibrations such as 1710 (guanine), 1661 (thymine), 1610 (adenine), 1491 (cytosine), and 1225 (PO_2^- asymmetric) cm^{-1} versus polymer concentrations were obtained after peak normalization using:

$$R_i = \frac{I_i}{I_{968}} \tag{1}$$

where I_i is the intensity of absorption peak for pure DNA and DNA in the complex with i concentration of polymer and I_{968} is the intensity of the 968 cm^{-1} peak (internal reference).[18]

CD Spectroscopy. Spectra of DNA and PEG−DNA adducts were recorded at pH 7.3 with a Jasco J-720 spectropolarimeter. For measurements in the far-UV region (200−320 nm), a quartz cell with a path length of 0.01 cm was used. Six scans were accumulated at a scan speed of 50 nm per minute, with data being collected at every nm from 200 to 320 nm. Sample temperature was maintained at 25 °C using a Neslab RTE-111 circulating water bath connected to the water-jacketed quartz cuvette. Spectra were corrected for buffer signal and conversion to the Mol CD ($\Delta\varepsilon$) was performed with the Jasco Standard Analysis software. The PEG concentrations used in our experiment were 0.125, 0.25, 0.5, and 1 mM with final DNA content of 2.5 mM (P).

Absorption Spectroscopy. The absorption spectra were recorded on a Perkin-Elmer Lambda 40 Spectrophotometer, with a slit of 2 nm and scan speed of 240 nm min^{-1}. Quartz cuvettes of 1 cm were used. The absorbance assessments were performed at pH 7.3 by keeping the concentration of DNA constant (125 μM), while varying polymer concentrations (5−80 μM).

To calculate the binding constant (k) for polymer−DNA complexes, it is assumed that the interaction between the ligand L and the substrate S is 1:1; for this reason, a single complex SL (1:1) is formed.[19] It was also assumed that the sites (and all the binding sites) are independent and finally Beer's law is followed by all species. A wavelength is selected at which the molar absorptivities ε_S (molar absorptivity of the substrate) and ε_{11} (molar absorptivity of the complex) are different. Then at total concentration S_t of the substrate, in the absence of ligand where the light path length is b = 1 cm, the solution absorbance is

$$A_o = \varepsilon_S b S_t \tag{2}$$

In the presence of ligand at total concentration L_t, the absorbance of a solution containing the same total substrate concentration is

$$A_L = \varepsilon_S b[S] + \varepsilon_L b[L] + \varepsilon_{11} b[SL] \tag{3}$$

(where [S] is the concentration of the uncomplexed substrate, [L] is the concentration of the uncomplexed ligand, and [SL] is the concentration of the complex) which, combined with the mass balance on S and L, gives

$$A_L = \varepsilon_S b S_t + \varepsilon_L b L_t + \Delta\varepsilon_{11} b[SL] \tag{4}$$

where $\Delta\varepsilon_{11} = \varepsilon_{11} - \varepsilon_S - \varepsilon_L$ (ε_L molar absorptivity of the ligand). By measuring the solution absorbance against a reference containing ligand at the same total concentration L_t, the measured absorbance becomes:

$$A = \varepsilon_S b S_t + \Delta\varepsilon_{11} b[SL] \tag{5}$$

Combining eq 4 with the stability constant definition K_{11} = [SL]/[S][L], gives:

$$\Delta A = K_{11}\Delta\varepsilon_{11} b[S][L] \tag{6}$$

where $\Delta A = A - A_o$. From the mass balance expression S_t = [S] + [SL] we get [S] = $S_t/(1 + K_{11}[L])$, which is eq 5, giving eq 6 at the relationship between the observed absorbance change per centimeter and the system variables and parameters.

$$\frac{\Delta A}{b} = \frac{S_t K_{11}\Delta\varepsilon_{11}[L]}{1 + K_{11}[L]} \tag{7}$$

Equation 6 is the binding isotherm, which shows the hyperbolic dependence on free ligand concentration.

The double-reciprocal form of plotting the rectangular hyperbola $1/y = f/d \times 1/x + e/d$, is based on the linearization of eq 6 according to the following equation:

$$\frac{b}{\Delta A} = \frac{1}{S_t K_{11}\Delta\varepsilon_{11}[L]} + \frac{1}{S_t\Delta\varepsilon_{11}} \tag{8}$$

Thus, the double reciprocal plot of $1/\Delta A$ versus $1/[L]$ is linear and the binding constant can be estimated by the

following equation:

$$K_{11} = \frac{intercept}{slope} \quad (9)$$

Fluorescence Spectroscopy. Fluorometric experiments were carried out on a Varian Cary Eclipse. Solutions of PEG−anthracence (80 μM) was prepared at 25 ± 1 °C. Various solutions of DNA (5−80 μM) in 10 mM Tris−HCl (pH. 7.4) were also prepared at 25 ± 1 °C. The fluorescence spectra were recorded at λ_{exc} = 330−350 nm and λ_{em} 390−450 nm related to anthracene fluoropore.[20] The intensity at 420 nm was used to calculate the binding constant (K) for PEG−anthracene−DNA adducts. Similar method has been used to calculate the binding constant of retinol and retinoic acid to DNA.[21]

On the assumption that there are (n) substantive binding sites for quencher (Q) on protein (B), the quenching reaction can be shown as follows:

$$nQ + B \leftrightarrow Q_nB \quad (10)$$

The binding constant (K_A), can be calculated as

$$K_A = [Q_nB]/[Q]^n[B] \quad (11)$$

where, [Q] and [B] are the quencher and polymer concentration, respectively, [Q_nB] is the concentration of non-fluorescent fluorophore−quencher complex, and [B_0] gives total polymer concentration:

$$[Q_nB] = [B_0] - [B] \quad (12)$$

$$K_A = ([B_0] - [B])/[Q]^n[B] \quad (13)$$

The fluorescence intensity is proportional to the polymer concentration as described:

$$[B]/[B_0] \propto F/F_0 \quad (14)$$

Results from fluorescence measurements can be used to estimate the binding constant of polymer−DNA complex. From eq 13:

$$\log[(F_0 - F)/F] = \log K_A + n \log[Q] \quad (15)$$

The accessible fluorophore fraction (f) can be calculated by modified Stern−Volmer equation:

$$F_0/(F_0 - F) = 1/fK[Q] + 1/f \quad (16)$$

where F_0 is the initial fluorescence intensity and F is the fluorescence intensities in the presence of quenching agent (or interacting molecule). K is the Stern−Volmer quenching constant, [Q] is the molar concentration of quencher, and f is the fraction of accessible fluorophore to a polar quencher, which indicates the fractional fluorescence contribution of the total emission for an interaction with a hydrophobic quencher.[14] The plot of $F_0/(F_0 - F)$ vs $1/[Q]$ yields f^{-1} as the intercept on y axis and $(fK)^{-1}$ as the slope. Thus, the ratio of the ordinate and the slope gives K.

Atomic Force Microscopy. Polymer−DNA complexes at a ratio of 1:1 and final DNA concentration of 0.1 mM were prepared in 5 mL tris-HCl (pH 7.4). The solutions were either used undiluted or diluted further in ultrapure water. For each sample, 30 μL aliquot was adsorbed for 2 min on freshly cleaved muscovite mica. The surface was rinsed thoroughly with 10 mL of ultrapure water and dried with Argon. AFM imaging was performed in acoustic mode at a scanning speed of 1 Hz with a Pico-AFM (Molecular Imaging, Phoenix, AZ) using high frequency (300 kHz) silicon cantilevers with a tip radius of 10 nm (TESP, Veeco, Santa Barbara, CA). Images were treated using the software Gwyddion (http://gwyddion.net/).

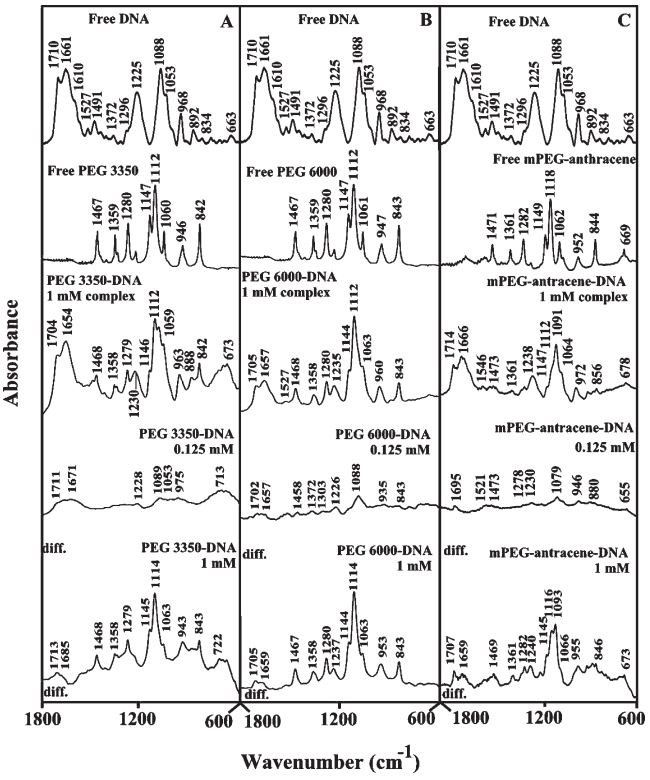

Figure 1. FTIR spectra and difference spectra [(DNA solution + PEG solution) -(DNA solution)] in the region of 1800−600 cm^{-1} for the free calf-thymus DNA and free PEG 3350 (A), free PEG 6000 (B), and free mPEG−anthracene (C) and their complexes in aqueous solution at pH 7.3 with various polymer concentrations (0, 125, and 1 mM) and constant DNA content (12.5 mM).

RESULTS AND DISCUSSION

FTIR Spectra of PEG−DNA Adducts. The IR spectral features for PEG 3350-, PEG 6000- and mPEG−anthracene−DNA complexes are presented in Figures 1 and 2.

PEG−Phosphate Binding. The PEG−PO_2 interaction was evident from an increase in the intensity and shifting of the PO_2 antiymmetric band at 1225 cm^{-1}[117,18,22−26] in the spectra of the polymer−DNA complexes (Figure 1, parts A, B, and C). The PO_2 band at 1225 cm^{-1} gained intensity and shifted toward higher frequencies at 1230 (PEG 3350), 1235 (PEG 6000) and 1238 (mPEG−anthracence), while the band at 1085 cm^{-1} related to the phosphate symmetric stretching vibration was overlapped by the strong polymer absorption band at 1112 (free PEG 3350), 1112 (free PEG 6000), and 1118 cm^{-1} (free mPEG−anthracene), which made it difficult to draw a certain conclusion on its position in the spectra of the polymer−DNA complexes (Figures 1 and 2, A, B, and C, complexes with 1 mM). Similarly, at low polymer concentration of 0.125 mM, the phosphate band at 1225 cm^{-1} exhibited a minor intensityy changes and shifting to a higher frequency at 1227 (PEG 3350), 1230 (PEG 6000) and 1232 cm^{-1} (mPEG−Anthracene) upon DNA complexation (spectra not shown).

dx.doi.org/10.1021/jp205079u |J. Phys. Chem. B 2011, 115, 9873–9879

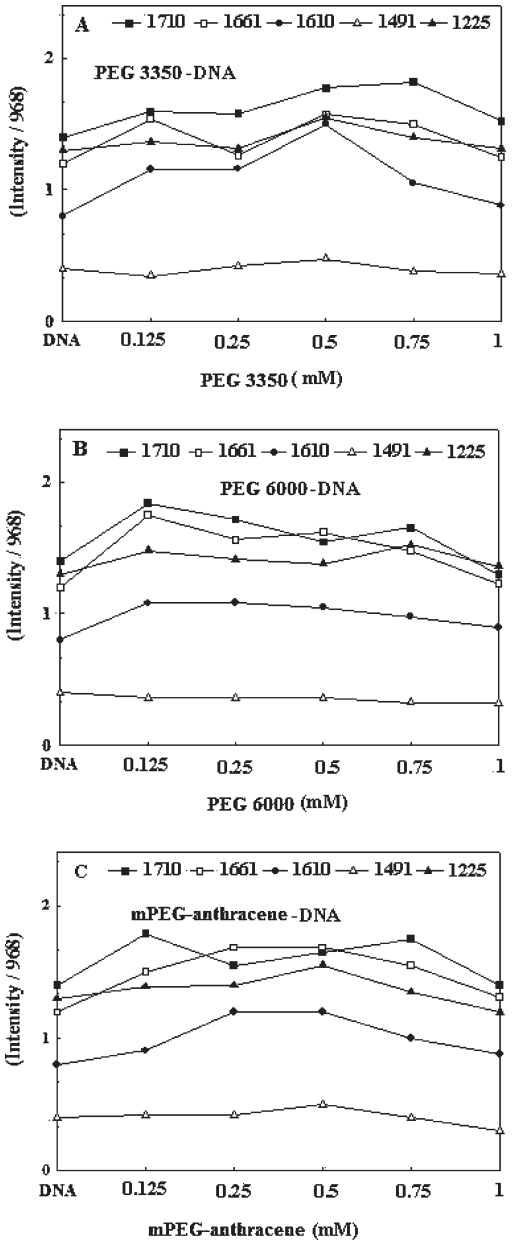

Figure 2. Intensity ratio variations for DNA infrared in-plane vibrations upon polymer complexation for (A) PEG 3350−DNA, (B) PEG 6000−DNA, and (C) mPEG−anthracene−DNA.

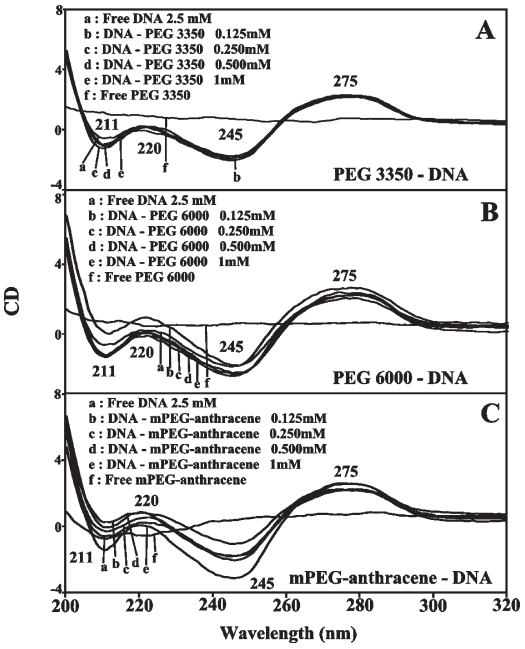

Figure 3. CD spectra of calf thymus DNA in Tris−HCl (pH ∼ 7.3) at 25 °C (2.5 mM) and PEG 3350 (A), PEG 6000 (B), and mPEG−anthracene (C) with 0.125, 0.25, 0.5, and 1 mM polymer concentrations.

The positive features at 1240−1230 cm^{-1} (PO_2 antisymmetric stretch) in the difference spectra of polymer−DNA complexes are due to an increase in the intensity of the phosphate vibrational frequencies, upon PEG interaction (Figures 1 and 2, A, B, and C differences, 0.125 and 1 mM). The larger shifting of the PO_2 band from 1225 to 1238 cm^{-1} in the spectrum of the mPEG−anthracene-−NA is indicative of a stronger polymer−phosphate interaction for mPEG−anthracene−DNA adduct (Figure 1).

PEG−Base Binding. Evidence for PEG−base binding comes from the spectral changes observed for free DNA upon polymer complexation. At low polymer concentration 0.125 mM, a minor shifting of the bands at 1710 (guanine) and 1661 (thymine) toward lower frequency was observed. The shifting was accompanied by a minor increase in intensity of the bands at 1710 (guanine) and 1661 cm^{-1} for the PEG−DNA complexes (Figure 2, parts A, B and C, 0125 mM). The increase in intensity of these vibrations was characterized by the presence of several weak positive features at 1711−1695 (guanine) and 1671−1657 (thymine) in the difference spectra of PEG 3350−, PEG 6000−, and mPEG−anthracence−DNA complexes (Figures 1 and 2, parts A, B and C, difference, 0.125 mM). The observed spectral changes are due to minor polymer−DNA interaction at low PEG concentration. As polymer concentration increased >0.125 mM, a gradual increase in intensities of base and phosphate vibrations were observed indicating of continuation of polymer interaction with DNA bases (Figure 2, parts A, B, and C). However at high polymer concentration 1 mM, major reduction in the intensity of base and PO_2 vibrations occurred, while the bands at 1710 (guanine) and 1661 cm^{-1} (thymine) shifted toward lower frequencies at 1704, 1654 (PEG 3350) and 1705, 1657 (PEG 6000) cm^{-1} and to a higher frequency at 1714 and 1666 cm^{-1} (mPEG−anthracence), upon DNA complexation (Figures 1 and 2, parts A, B and C, complexes 1 mM). The shift of these vibrations to higher frequencies in the spectrum of mPEG−anthracene−DNA adduct is indicative of different binding modes of mPEG−anthracene with respect to PEG-3350 and PEG 6000. This is consistent with the AFM imaging results that showed weaker interaction for mPEG−anthracene (will be discussed further on). However, the decrease in intensity of DNA base vibrations observed at high polymer content (1 mM) is due to DNA condensation and particle formation (Figure 2), which is consistent with the CD results discussed below. Similar aggregation and particle formation were observed for DNA upon dendrimer complexation.[10] The increase in the intensity and the shifting of these vibrations are due to polymer-base interaction via guanine N7 and thymine O2 atoms in these

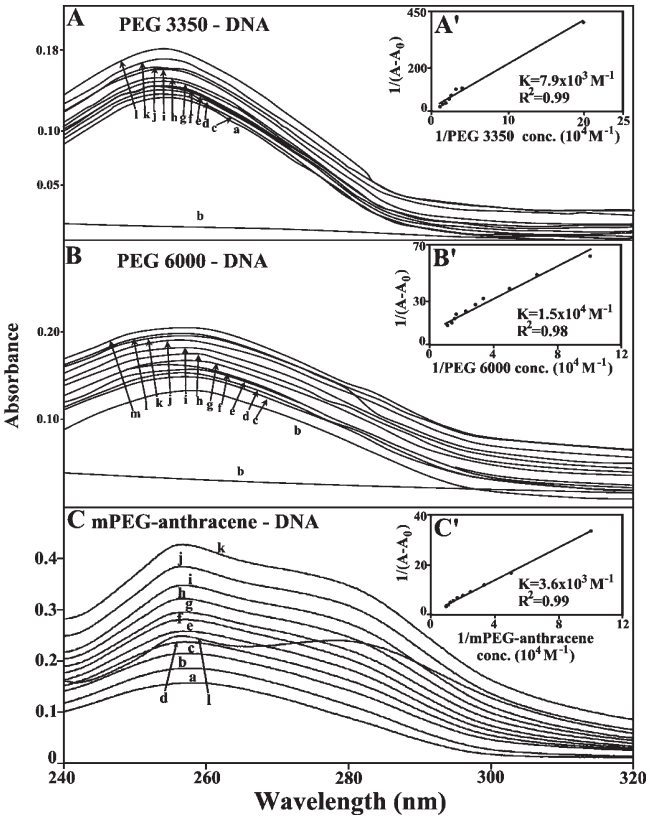

Figure 4. UV−visible results of calf-thymus DNA and its PEG 3350 (A), PEG 6000 (B), and mPEG−anthracene (C) complexes: (A) spectra of (a) free DNA (40 μM); (b) free PEG 3350 (100 μM); (c−l) PEG 3350−DNA complexes c (5), d (10), e (15), f (20), g (25), h (30), i (35), j (40), k (50), and l (60). (B) spectra of (a) free DNA (40 μM); (b) free PEG 6000 (100 μM); (c−m) PEG 6000−DNA complexes c (5), d (10), e (15), f (20), g (25), h (30), i (35), j (40), k (50), l (60), and m (80). (C) spectra of (a) free DNA (40 μM); (b) free mPPEG−anthracene (100 μM); (c−k) mPEG−anthracene−DNA complexes c (5), d (10), e (20), f (30), g (40), h (50), i (60), j (70), and k (80 μM). Plot of $1/(A - A_0)$ vs (1/polymer concentration) for K calculation of polymer and calf-thymus DNA complexes, where $A0$ is the initial absorbance of DNA (260 nm) and A is the recorded absorbance (260 nm) at different polymer concentrations (5−80 μM) with constant DNA concentration of 100 μM at pH 7.4 for PEG 3350 (A′), PEG 6000 (B′), and mPEG−anthracene (C′).

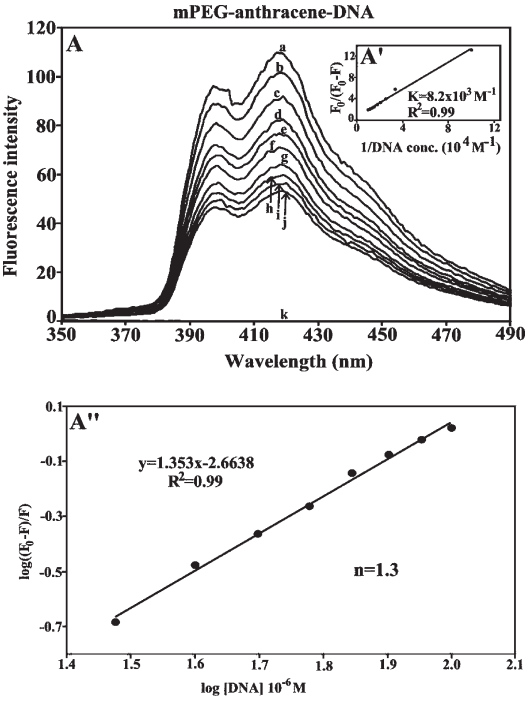

Figure 5. Fluorescence emission spectra of mPEG−anthracene−DNA systems in 10 mM Tris−HCl buffer pH 7.4 at 25 °C for (A) polymer−DNA: (a) free mPEG−anthracene (80 μM), (b−j) with polymer−DNA complexes at 5, 10, 15, 20, 30, 40, 60, 80, and 100 μM with (k) free DNA 100 μM. The plot of $F_0/(F_0 - F)$ as a function of 1/DNA concentration. The binding constant K being the ratio of the intercept and the slope for (A′) mPEG−anthracene−DNA. The plot of log $(F_0 - F)/F$ as a function of log [DNA] for calculation of number of bound mPEG−anthracene molecules per DNA (n) in polymer−DNA complexes (A″).

polymer−DNA complexes, while the reduction of intensity of these bands is related to a major DNA condensation in the presence PEG and mPEG−anthracene.

CD Spectra and DNA Conformation. The CD spectra of the free DNA and its PEG complexes with different polymer concentrations are shown in Figure 3. The CD of the free DNA composed of four major peaks at 211 (negative), 220 (positive), 245 (negative), and 275 nm (positive) (Figure 3). This is consistent with CD spectra of double helical DNA in B conformation.[27,28] Upon PEG interaction no major shifting of the CD bands was observed at low polymer concentration (0.125 to 0.25 mM), whereas, at higher polymer content (0.5 and 1 mM), a major increase in molar ellipticity of the band at 211 nm was observed, while the negativity of the band at 245 nm increased and the intensity of the band at 275 nm decreased in the spectra of PEG 3350−, PEG 6000−, and mPEG−anthracene−DNA adducts (Figure 3, parts A, B, and C). The loss of intensity of the CD band at 275 nm and the intensity variations of the band at 211, 220, and 245 nm in the spectra of polymer−DNA complexes are due to DNA condensation in the presence of PEGs and mPEG−anthracene (Figure 3, parts A, B and C). This is consistent with our AFM images that will be discussed further on. Similar DNA condensation and aggregation were observed in the presence of dendrimers and cationic lipids.[10,22] The CD results are also consistent with our infrared data on the PEG−DNA complexes that showed no conformational changes for B−DNA with marker bands at 1710 (G), 1225 (PO_2), and 834 cm^{-1} (phosphodiester mode) (Figure 1, parts A, B, and C). The shifting of the guanine bands at 1710 cm^{-1} to lower frequency and the PO_2 band at 1225 cm^{-1} to higher frequency is due to polymer interaction with guanine N7 site and the backbone phosphate group and not due to DNA conformational transition, since the phosphodiester band at 834 cm^{-1} showed no major shifting in the spectra of the polymer−DNA complexes (Figure 1, parts A, B, and C) consistent with our CD results discussed above (Figure 3).

Hydrophobic Contacts. To determine the presence of hydrophobic contact in the PEG−DNA complexes, the spectral changes of the polymer antisymmetric and symmetric CH_2 stretching vibrations, in the region of 3000−2800 cm^{-1} were examined by infrared spectroscopy. The CH_2 bands of the free PEG 3350 located at 2944 and 2859 cm^{-1} shifted to 2946, 2885, and 2855 cm^{-1} (PEG 3350−DNA); free PEG 6000 with CH_2 bands at 2944, 2883, and 2859 cm^{-1} shifted (only for one band) to 2854 cm^{-1} (PEG 6000−DNA) and free mPEG−anthracence

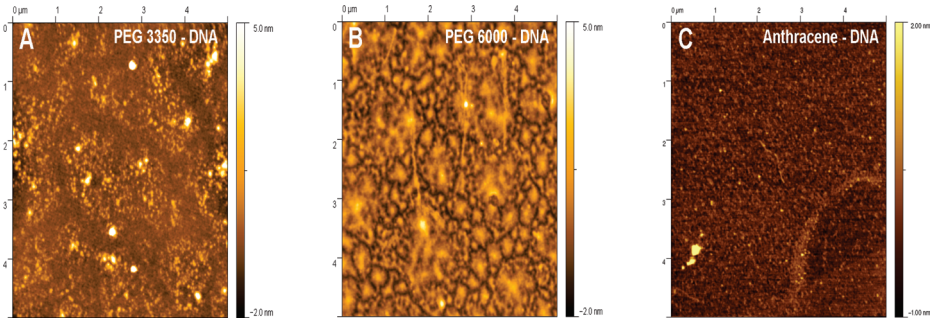

Figure 6. Tapping mode AFM pictures in air of PEG−DNA complexes diluted 10 or 100 times in ultrapure water and adsorbed to mica. (A) the PEG 3350 sample showed poorly condensed DNA molecules. (B) Complexes obtained with PEG 6000 had mainly a "fried egg" morphology as observed previously for DOTAP−DNA mixtures. (C) Typical image obtained for the mPEG−anthracene sample showing no clear evidence of complexation.

with CH_2 bands at 2944, 2883, and 2857 cm^{-1} shifted to 2942, 2881, and 2859 cm^{-1} (mPEG−anthracene−DNA) in these polymer−DNA complexes (spectra not shown). The shifting of the polymer antisymmetric and symmetric CH_2 stretching vibrations in the infrared spectra the polymer−DNA complexes suggests the presence of hydrophobic interactions via polymer aliphatic chain and hydrophobic region in DNA.

Stability of PEG−DNA Complexes. The dendrimer−DNA binding constant was determined as described in Materials and Methods (UV−visible spectroscopy). An increasing polymer concentration resulted into an increase in UV light absorption, as can be observed (Figure 4). This is consistent with a reduction of base stacking interaction due to polymer complexation (Figure 4A, 4B and 4C). The double reciprocal plot of $1/(A - A_0)$ vs 1/(polymer concentration) is linear and the binding constant (K) can be estimated from the ratio of the intercept to the slope (Figure 4A′, 4B′ and 4C′). A_0 is the initial absorbance of the free DNA at 260 nm and A is the recorded absorbance of complexes at different polymer concentrations. The overall binding constants for PEG−DNA complexes are estimated to be $K_{PEG\ 3350} = 7.9\ (\pm 1) \times 10^3\ M^{-1}$, $K_{PEG\ 6000} = 1.5\ (\pm 0.4) \times 10^4\ M^{-1}$, and $K_{mPEG-anthracene} = 3.6\ (\pm 0.8 \times 10^3\ M^{-1}$ with the order of stability of polymer−DNA complexes being PEG 6000 > mPPEG 3350 > mPEG−anthracene (Figure 4A′, 4B′ and 4C′). Similar binding constants were observed for other polymer−DNA complexes.[10] The binding constants estimated are mainly due to the polymer-base binding and not related to the polymer-PO_2 interaction, which is largely ionic and can be dissociated easily in aqueous solution.

Fluorescence Spectra and Stability of mPEG−Anthracene−DNA Adduct. Since DNA is a weak fluorophore, the titration of mPEG−anthracene was done against various DNA concentrations, using mPEG−anthracene excitation at 330−350 nm and emission at 400−450 nm.[20] When mPEG−anthracene interacts with DNA, fluorescence may change depending on the impact of such interaction on the mPEG−anthracence conformation, or via direct quenching effect. The decrease of fluorescence intensity of mPEG−anthracence has been monitored at 420 nm for mPEG−anthracence−DNA systems. The plot of $F_0/(F_0 - F)$ vs 1/[DNA] is shown in Figure 5A. Assuming that the observed changes in fluorescence come from the interaction between mPEG−anthracene and polynucleotides, the quenching constant can be taken as the binding constant of the complex formation. The K value given here is averages of four-replicate and six-replicate runs for mPEG−anthracence−DNA systems, each run involving several different concentrations of DNA (Figure 5A). The binding constant obtained was $K_{mPEG-anthracene-DNA} = 8.2\ (\pm 1) \times 10^3\ M^{-1}$ (Figure 4A′). The association constant calculated for the mPEG−anthracene−DNA adduct suggests low affinity mPEG−anthracence-polynucleotide binding. The f values obtained in Figure 5, suggest that DNA also interact with fluorophore via hydrophobic interactions, which is consistent with our infrared spectroscopic results discussed above (Hydrophobic Contacts).

The number of mPEG−anthracene molecules bound per polynucleotides (n) is calculated from $\log [(F_0 - F)/F] = \log K_S + n \log[\text{DNA}]$ for the static quenching.[21,29,30] The linear plot of $\log [(F_0 - F]/F]$ as a function of log [DNA] is shown in Figure 5A″. The n values from the slope of the straight line 1.3 for mPEG−anthracene−DNA adduct (Figure 5A″).

Ultrastructure of PEG−DNA Complexes. The two PEG samples showed clear evidence of complexation by AFM imaging (Figure 6, parts A and B). However, this was not the case for the mPEG−Anthracene sample were naked DNA strands could be observed on the mica surface (Figure 6C). For the PEG 3350 sample, the complexation was not complete with the presence of DNA strands with a beaded appearance (Figure 6B). For the PEG 6000 sample, the complexation was much more extensive. The surface was covered with "fried-egg" aggregates similar to the ones observed previously for DOTAP−DNA mixtures.[22] The PEG 6000 complexes had an average height of 7.4 ± 0.2 nm (n = 904) and an average volume of 390000 ± 6600 nm^3 (n = 904). This is twice the height and five times the volume of an average DOTAP−DNA aggregate.[22]

■ CONCLUDING REMARKS

On the basis of our AFM imaging and spectroscopic results, PEG and mPEG−anthracene bind DNA via hydrophilic and hydrophobic interactions. Extensive complexation occurs for PEG 6000 with the order of stability of complex formation PEG 6000 > PEG 3350 > mPEG−anthracene. Major DNA condensation and particle formation occur at high polymer concentration, while DNA remains in B-conformation. The extent of DNA condensation was similar to those of cationic lipid−DNA complexes. PEG and its derivatives can be used to transport DNA in gene delivery system.

■ AUTHOR INFORMATION

Corresponding Author

*Telephone: 819-376-5011 (ext. 3310). Fax: 819-376-5084. E-mail: tajmirri@uqtr.ca.

■ ACKNOWLEDGMENT

This work is supported by grants from the Natural Sciences and Engineering Research Council of Canada (NSERC).

■ ABBREVIATIONS

PEG, poly(ethylene glycol); mPEG, methoxypoly(ethylene glycol); PAMAM, poly(amidoamine); A, adenine; G, guanine; C, cytosine; T, thymine; CD, circular dichroism; FTIR, Fourier transform infrared; AFM, atomic force microscopy

■ REFERENCES

(1) Bello-Roufai, M.; Lambert, O.; Pitard, B. *Nucleic Acids Res.* **2007**, *35*, 728–739.
(2) Kim, W.; Yamasaki, Y.; Jang, W. D.; Kataoka, K. *Biomacromolecules* **2010**, *11*, 1180–1186.
(3) Wang, R.; Zhou, L.; Zhou, Y.; Li, G.; Zhu, X.; Gu, H.; Jiang, X.; Li, H.; Wu., J.; He, L.; Guo, X.; Zhu, B.; Yan, D. *Biomacromolecules* **2010**, *11*, 489–495.
(4) Fant, K.; Esbjorner, E. K.; Jenkins, A.; Grossel, M. C.; Lincoln, P.; Norden, B. *Mol. Pharmaceutics* **2010**, *7*, 1743–1746.
(5) Yuan, Q.; Yeudall, W. A.; Yang, H. *Biomacromolecules* **2010**, *11*, 1940–1947.
(6) Luo, D.; Haverstick, K.; Belcheva, N.; Han, E.; Saltzman, W. M. *Macromolecules* **2002**, *35*, 3456–3462.
(7) Casettari, L.; Vllasaliu, D.; Mantovani, G.; Howdle, S. M.; Stolnik, S.; Illum, L. *Biomacromolecules* **2010**, *11*, 2854–2865.
(8) Lis, J. T.; Schlief, R. *Nucleic Acids Res.* **1975**, *2*, 383–389.
(9) Kimpton, C. P.; Corbitti, G.; Morris, D. J. *J. Virol. Methods* **1990**, *28*, 141–145.
(10) Froehlich, E.; Mandeville, J. S.; Weinert, C. M.; Kreplak, L.; Tajmir-Riahi, H. A. *Biomacromolecules* **2011**, *12*, 511–517.
(11) Froehlich, E.; Mandeville, J. S.; Weinert, C. M.; Kreplak, L.; Tajmir-Riahi, H. A. *Biomacromolecules* **2011**, *12*, 2780–2787.
(12) Froehlich, E.; Jennings, C. J.; Sedaghat-Herati, M. R.; Tajmir-Riahi, H. A. *J. Phys. Chem. B.* **2009**, *113*, 6986–6993.
(13) Mandeville, J. S.; Tajmir-Riahi, H. A. *Biomacromolecules* **2010**, *11*, 465–472.
(14) Lakowicz, J. R. *In Principles of Fluorescence Spectroscopy*, 3nd ed; Springer: New York, 2006.
(15) Reichmann, M. E.; Rice, S. A.; Thomas, C. A.; Doty., P. *J. Am. Chem. Soc.* **1954**, *76*, 3047–3053.
(16) Vijayalakshmi, R.; Kanthimathi, M.; Subramanian., V. *Biochem. Biophys. Res. Commun.* **2000**, *271*, 731–734.
(17) Alex, S.; Dupuis, P. *Inorg. Chim. Acta* **1989**, *157*, 271–281.
(18) Ahmed Ouameur, A.; Tajmir-Riahi, H. A. *J. Biol. Chem.* **2004**, *279*, 42041–42054.
(19) Connors, K. Binding constants: *The measurement of molecular complex stability*; John Wiley & Sons: New York, 1987.
(20) del Vale, J. C.; Turek, A. M.; Tarakalanov, N. D.; Saltiel, J. *J. Phys. Chem. A* **2002**, *106*, 5101–5104.
(21) Mandeville, J. S.; N'soukpoé-Kossi, C. N.; Neault, J. F.; Tajmir-Riahi, H. A. *Biochem. Cell Biol.* **2010**, *88*, 469–477.
(22) Marty, R.; N' soukpoe-Kossi, C. N.; Charbonneau, D.; Weinert, C. M.; Kreplak, L.; Tajmir-Riahi, H. A. *Nucleic Acids Res.* **2009**, *37*, 849–857.
(23) Andrushchenko, V. V.; Leonenko, Z.; van de Sande, H.; Wieser, H. *Biopolymers* **2002**, *61*, 243–260.
(24) Dovbeshko, G. I.; Chegel, V. I.; Gridina, N. Y.; Repnytska, O. P.; Shirshov, Y. M.; Tryndiak, V. P.; Todor, I. M.; Solyanik, G. I. *Biopolymers (Biospectroscopy)* **2002**, *67*, 470–486.
(25) Loprete, D. M.; Hartman, K. A. *Biochemistry* **1993**, *32*, 4077–4082.
(26) Taillandier, E.; Liquier, J. *Methods Enzymol.* **1992**, *211*, 307–335.
(27) Vorlickova, M. *Biophys. J.* **1995**, *69*, 2033–2043.
(28) Kypr, J.; Vorlickova, M. *Biopolymers* **2002**, *67*, 275–277.
(29) Charbonneau, D. M.; Tajmir-Riahi, H. A. *J. Phys. Chem. B* **2010**, *114*, 1148–1155.
(30) Mandeville, J. S.; Tajmir- Riahi, H. A. *Biomacromolecules* **2010**, *11*, 465–472.